Bioconjugate Chemistry

Article

pubs.acs.org/bc

Development of a Clickable Designer Monolignol for Interrogation of Lignification in Plant Cell Walls

Natalie Bukowski,[†] Jyotsna L. Pandey,[‡,§] Lucas Doyle,[†] Tom L. Richard,[‡,§] Charles T. Anderson,[‡,#] and Yimin Zhu*[,†]

[†]Department of Chemistry, Altoona College, The Pennsylvania State University, Altoona, Pennsylvania 16601, United States

[‡]Center for Lignocellulose Structure and Formation, [§]Department of Agricultural and Biological Engineering, and [#]Department of Biology, The Pennsylvania State University, University Park, Pennsylvania 16802, United States

Supporting Information

ABSTRACT: Lignin is an abundant and essential polymer in land plants. It is a prime factor in the recalcitrance of lignocellulosic biomass to agricultural and industrial end-uses such as forage, pulp and papermaking, and biofuels. To better understand lignification at the molecular level, we are developing a lignin spectroscopic and imaging toolbox on one "negligible" auxiliary. Toward that end, we describe the design, synthesis, and characterization of a new designer monolignol, 3-*O*-propargylcaffeyl alcohol, which contains a bioorthogonal alkynyl functional group at the 3-*O*-position. Importantly, our data indicate that this monolignol does not alter the fidelity of lignification. We demonstrate that the designer monolignol provides a platform for multiple spectroscopic and imaging approaches to reveal temporal and spatial details of lignification, the knowledge of which is critical to reap the potential of energy-rich renewable plant biomass for sustainable liquid fuels and other diverse economic applications.

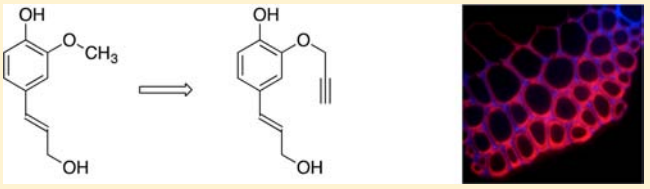

INTRODUCTION

Lignins are complex and irregular phenolic biopolymers, derived primarily from monolignols.[1−3] Essential to vascular plants, lignins interweave with polysaccharides to form a strong and hydrophobic cell wall matrix, which confers mechanical strength and facilitates water transport to support the upright growth of land plants in a gravitropic environment, and also helps protect plants against pathogens.[3,4] Lignin is a major factor in the recalcitrance of plant cell walls to degradation, making processing of plant-derived biomass difficult for a variety of natural and industrial applications, such as ruminant forage, pulp and papermaking, and lignocellulosic biofuels. As a result, lignin has attracted significant research interest as a target for reduction, enhanced degradability, and/or repurposing as a valuable coproduct.[5−11]

Lignification, the biological process of lignin polymerization and deposition, involves complex metabolic, transport, and chemical processes. Monolignols are first synthesized in the cytosol via a multienzyme pathway that starts with phenylalanine.[3,12,13] They are then transported across the plasma membrane to the apoplast, or extracellular space, where they undergo radical-mediated combinatorial polymerization and deposition to form insoluble lignin.[14,15] Despite much progress through genetic and structural studies, many molecular details of lignification remain elusive;[3,16] for example, how monolignols are transported across cell membranes is still under debate.[14,15] While recent studies suggest that some monolignol transport is mediated by ATP-binding cassette-like transport proteins,[17,18] accommodation of a wide range of natural and nonnatural lignin monomers during lignification indicates the presence of other transport routes.[9,14,19] Extensive evidence demonstrates that lignification is tightly regulated in vivo,[14,20,21] but how this process is spatially and temporally controlled is largely unknown. New chemical and biochemical tools are sorely needed to address these and other important research questions.

Spectroscopic and imaging approaches have become increasingly powerful tools in the quest to understand biological processes at the subcellular scale.[22−26] Such approaches have been developed to study events involving a variety of biological polymers, including but not limited to proteins, DNA, and carbohydrates.[23,27−30] Recently, designer monolignols for lignin research have begun to be developed. Ralph and co-workers have developed fluorophore-tagged monolignols that have been used to reveal the molecular details of lignification.[31,32] Theoretically, the same concept can be extended to develop designer monolignols equipped with other spectroscopic and imaging tags, which will allow for the use of complementary spectroscopic and imaging methods to elucidate the complexities of the lignification process. However, many tags are larger than the monolignols themselves (Figure 1) and may therefore dramatically alter the biological activity and subcellular localization of the monolignols to which they are attached. Evidence that fluorophores can change the distribution of tagged monolignols has been reported recently

Received: September 1, 2014
Revised: November 14, 2014
Published: November 18, 2014

   dx.doi.org/10.1021/bc500411u | *Bioconjugate Chem.* 2014, 25, 2189−2196

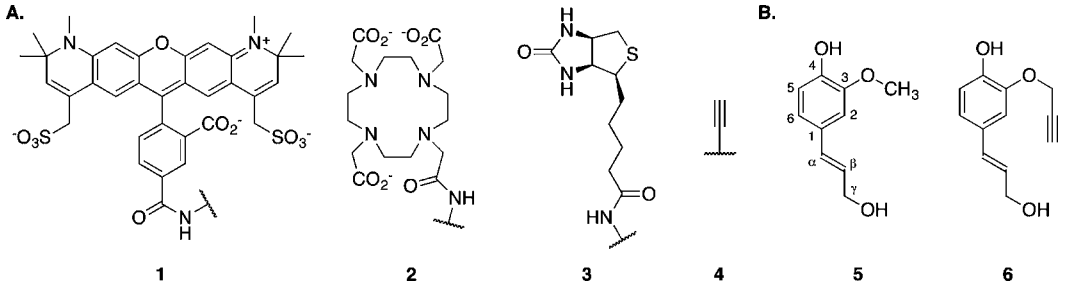

Figure 1. Chemical structures of several spectroscopic probes and monolignols. (A) Alexa 594, **1**, for fluorescence imaging; 1,4,7,10-tetraazacyclododecane-1,4,7,10-tetraacetic acid, **2**, for magnetic resonance imaging; biotin, **3**; and a terminal alkyne, **4**, which is the tag used in this paper; (B) coniferyl alcohol (CA), **5**; and 3-*O*-propargylcaffeyl alcohol, **6**, the designer monolignol developed in this paper.

in a study in which the authors used fluorescent monolignols to monitor lignification in vitro and in plant tissue.[33]

To develop a lignin spectroscopic and imaging toolbox on one "negligible" auxiliary, we report the design, synthesis, and initial application of 3-*O*-propargylcaffeyl alcohol as a designer monolignol and versatile analog of coniferyl alcohol (CA) for analysis of lignification (Figure 1B). Replacing the 3-*O*-methyl group with a propargyl group introduces a "negligible" perturbation, and this small bioorthogonal group serves as a general platform for different spectroscopic and imaging approaches.

Scheme 1. Synthesis of 3-*O*-Propargylcaffeyl Alcohol, 6

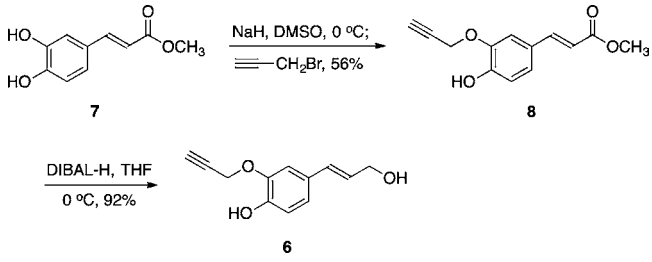

RESULTS AND DISCUSSION

Design and Synthesis of 3-*O*-Propargylcaffeyl Alcohol. In designing a general platform for experimental interrogation of lignification, we sought to attach a small bioorthogonal tag to a monolignol: once incorporated into lignins, this tag will allow for the use of versatile bioorthogonal chemistry to introduce various spectroscopic and imaging probes for further studies.[34] Specifically, a terminal alkyne was selected as a tag of choice because of its small size, its compatibility with robust click chemistry that has been used to image glycans in plants and other organisms,[30,34−37] and its potential to generate a significant Raman scattering signal in a silent region of the cellular Raman spectrum.[38,39] To link a terminal alkyne moiety to coniferyl alcohol, we chose to avoid making any direct modification of aryl/alkenyl carbons, which can alter the redox potential of the phenol and thus might have a significant impact on lignification.[40] The γ-*O*-positions of monolignols have previously been used as modification sites in designing new lignin monomers.[9,11,41,42] However, due to the loss of the γ-OH, such modifications can produce tetrahydrofuran-type $\beta-\beta$-interunit linkages instead of the typical $\beta-\beta$-linkages, as previously reported for lignification involving γ-acylated monolignols.[43] Although no monolignol with modification (other than isotopic ones) at the 3-*O*-methyl has previously been investigated as a lignin precursor, we hypothesized that replacing the 3-*O*-methyl group with a small alkyl group would neither significantly alter the redox potential of the phenol nor introduce new interunit linkages. Following these considerations, we designed 3-*O*-propargylcaffeyl alcohol as a coniferyl alcohol analog for this study (Figure 1B).

The synthesis of 3-*O*-propargylcaffeyl alcohol started from the regioselective alkylation of methyl caffeate (Scheme 1). The hydroxyl groups of methyl caffeate were deprotonated by adding excess sodium hydride. The less acidic 3-hydroxyl group generated the more nucleophilic phenoxide, which was selectively alkylated to produce methyl 3-*O*-propargylcaffeate in 56% yield. The ester was then reduced by diisobutylaluminum hydride to generate the desired 3-*O*-propargylcaffeyl alcohol in 92% yield.

Horseradish Peroxidase-Catalyzed Dehydrogenative Polymerization. As a potential probe for lignification, it is important to determine whether the designer monolignol is compatible with lignification, i.e., whether it can undergo enzyme-initiated oxidation and participate in subsequent radical coupling, particularly cross-coupling with naturally occurring monomers into lignins. Indeed, we found that 3-*O*-propargylcaffeyl alcohol readily undergoes oxidative coupling in the conventional horseradish peroxidase (HRP)$-H_2O_2$ system. To test the fidelity of 3-*O*-propargylcaffeyl alcohol in lignification, we produced synthetic lignins (DHPs) using 3:1 coniferyl alcohol/3-*O*-propargylcaffeyl alcohol with HRP and H_2O_2 in the presence of a catalytic amount (2 mol %) of methyl *p*-coumarate. The structural compositions of the DHPs were determined using 2D heteronuclear single quantum coherence NMR spectroscopy (HSQC-NMR, Figure 2). The NMR spectrum of the DHP copolymers with 3-*O*-propargylcaffeyl alcohol is similar to that of DHP polymers generated with only coniferyl alcohol, with typical β-O-4-, β-5-, and $\beta-\beta$-substructures as the major interunit linkages. Only two new peaks, which correspond to the two C−H signals of the propargyl side chains, were observed in the NMR spectrum of the DHP copolymers. These results suggest that 3-*O*-propargylcaffeyl alcohol is incorporated into synthetic lignins with the propargyl group intact and does not alter the fidelity of in vitro lignification.

With the terminal alkyne groups incorporated into lignins, we next performed Raman spectroscopic analysis on the DHP copolymers. Although alkynes have been well-characterized as spectroscopic and imaging tools by coupling with other reporters through bioorthogonal reactions (see below), we were also interested in identifying unique spectroscopic properties of the DHP copolymers that could be useful for future studies. As expected, the Raman spectrum of the DHP copolymers with 3-*O*-propargylcaffeyl alcohol is very similar to

dx.doi.org/10.1021/bc500411u | *Bioconjugate Chem.* 2014, 25, 2189−2196

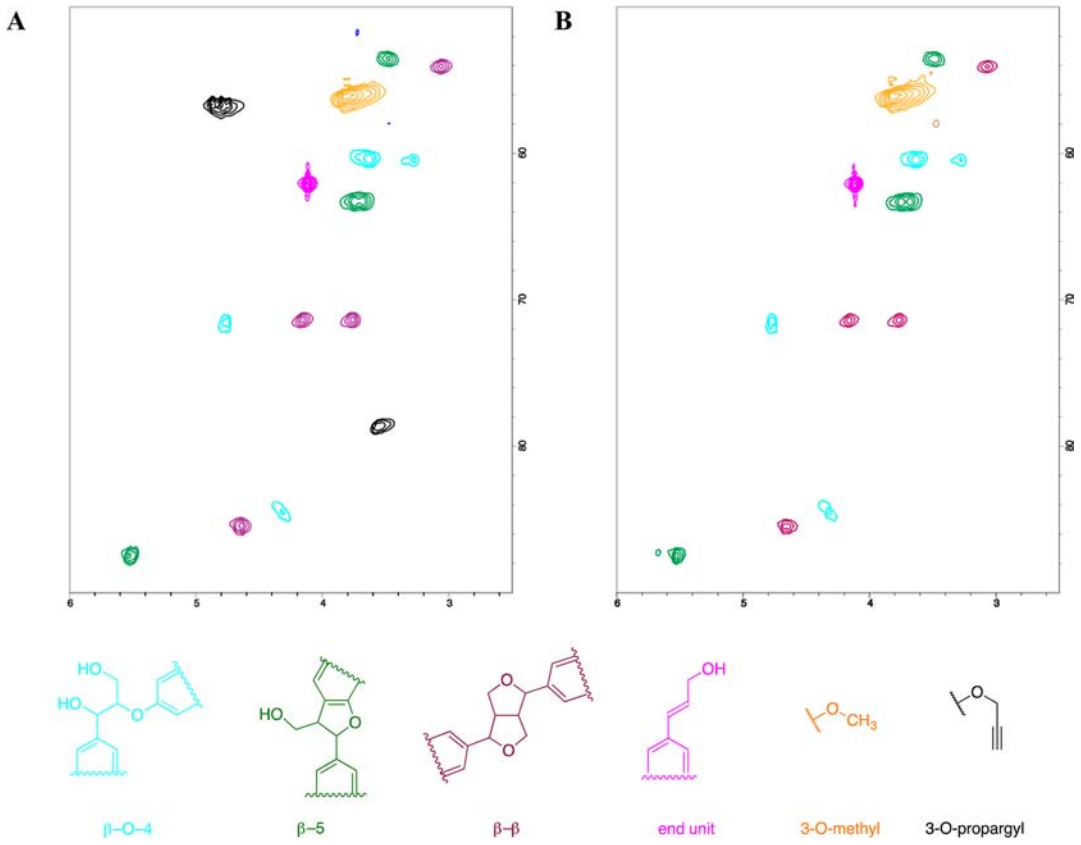

Figure 2. Aliphatic regions of the HSQC 2D-NMR spectra of (**A**) DHP copolymers of 3:1 CA/**6** and (**B**) DHP polymers of CA.

that of the DHP polymers containing only coniferyl alcohol, with the exception of an additional significant scattering peak at 2100 cm^{-1}, which corresponds to the alkynyl stretching vibration (Figure 3). Interestingly, this peak falls in a cellular silent region, where most endogenous molecules show no Raman scattering signals.[38,39] We envision that the incorporation of 3-*O*-propargylcaffeyl alcohol into lignins should enable direct detection of lignification in plant cell walls through Raman imaging, without introducing additional spectroscopic reporters.[24,39]

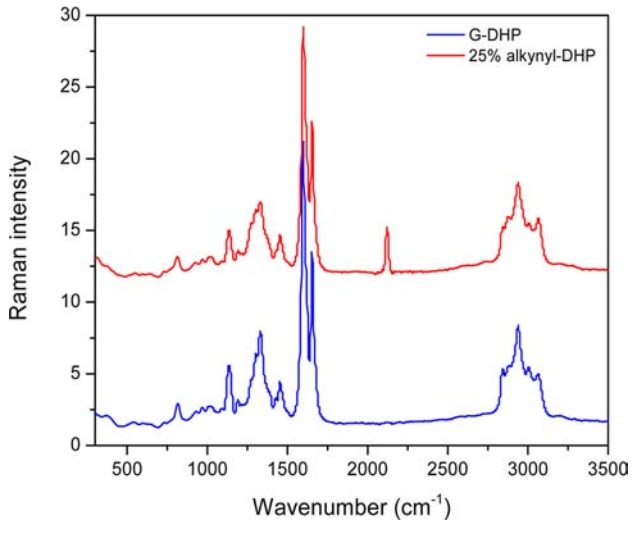

Figure 3. Raman spectra of synthetic lignins, DHP polymers with CA (blue trace), and DHP copolymers with 3:1 CA/**6** (red trace). The copolymers (red) show a characteristic alkyne peak at 2100 cm^{-1}. The two spectra are stacked with the red spectrum shifted by separation of 10 units.

Incorporation in *Arabidopsis* Tissues. As an initial example of using our designer monolignol to perform molecular analysis of lignification in plants, we performed feeding experiments using live *Arabidopsis* Col-0 seedlings. Four-day-old seedlings were incubated in liquid Murashige and Skoog (MS) medium containing 3-*O*-propargylcaffeyl alcohol and/or coniferyl alcohol for 4 h. To demonstrate the flexibility of 3-*O*-propargylcaffeyl alcohol as a platform for imaging, we chose to exploit click-chemistry-enabled fluorescence imaging for detection of incorporation of the monolignol. After incorporation, seedlings were treated with Alexa 594-azide in the presence of copper(II) sulfate and ascorbic acid to fluorescently tag any incorporated alkynyl groups, followed by imaging using spinning disk confocal fluorescence microscopy. Seedlings treated with the designer monolignol displayed significant fluorescence throughout the root tissues (Figure 4B, C, E, F), whereas no visible fluorescence was observed in control seedlings treated with only coniferyl alcohol (Figure 4A and D). In seedlings treated with 3-*O*-propargylcaffeyl alcohol, fluorescence intensity increased progressing from the root tip to the differentiation zone, with maximum intensity observed in the late differentiation zone (Figure 4E and F). Seedlings treated with 3:1 coniferyl alcohol/3-*O*-propargylcaffeyl alcohol (Figure 4E) exhibited lower fluorescence intensity than seedlings treated only with 3-*O*-propargylcaffeyl alcohol (Figure 4F), the difference being most apparent in the late differentiation zone. Incorporation in these tissues was observed in similar studies that applied coniferyl alcohol and fluorophore-tagged coniferyl alcohols in feeding experiments.[20,32] These

dx.doi.org/10.1021/bc500411u | *Bioconjugate Chem.* 2014, 25, 2189−2196

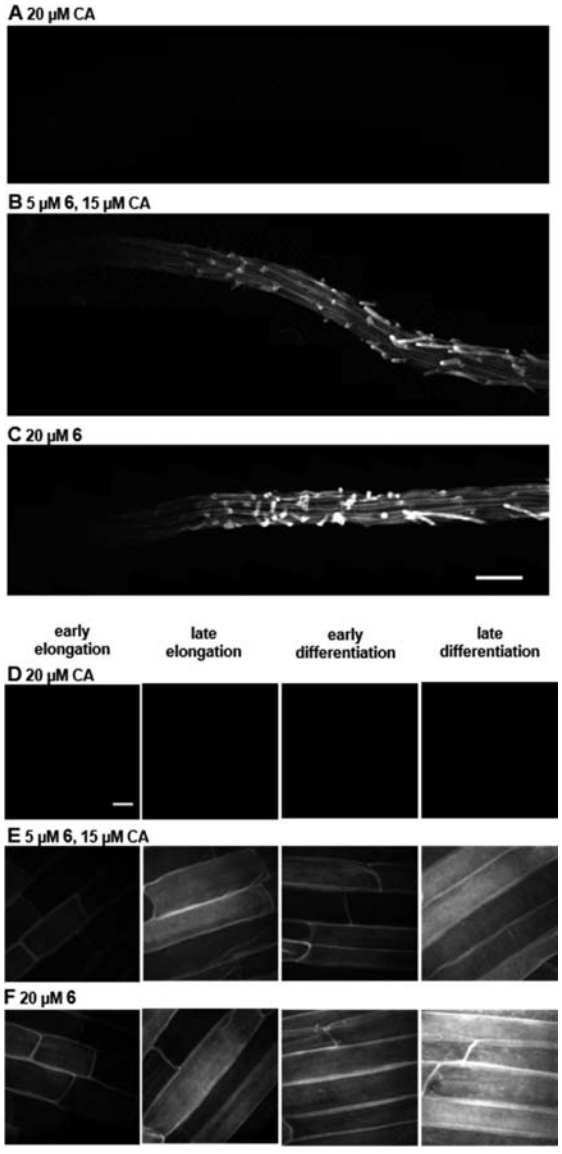

Figure 4. Images of 3-*O*-propargylcaffeyl alcohol's incorporation into roots of 4 day old *Arabidopsis* seedlings. (A,D) control seedlings treated with 20 μM CA. (B,E) seedlings treated with 5 μM 3-*O*-propargylcaffeyl alcohol, **6**, and 15 μM CA. (C,F) seedlings treated with 20 μM **6**. Images were collected with a spinning disk fluorescence confocal microscope using a 561 nm laser at 10% power and 500 gain with an exposure time of 400 ms. (A–C) Contrast-enhanced mosaics of contiguous images, starting at the root tip (left) and going through the late differentiation zone (right), recorded using a 20× objective (Scale bar, 100 μm). (D–F) Contrast-enhanced maximum intensity projections of *z* series recorded at the indicated root zones with a 100× oil-immersion objective (Scale bar, 10 μm).

results demonstrate that our designer monolignol was successfully incorporated into at least the surface tissues of roots of four-day-old *Arabidopsis* seedlings and then fluorescently labeled via a copper-catalyzed click reaction. We note that copper-catalyzed click labeling is also affected by the potential of the corresponding dyes to penetrate tissues. While the similarity to coniferyl alcohol makes it likely that 3-*O*-propargylcaffeyl alcohol is able to penetrate deep into the root tissue, we observed that the penetration of the charged Alexa 594-azide into the interior of *Arabidopsis* roots was low and no fluorescence was observed in the endodermis, Casparian strips, or the vasculature, which are typically lignifying tissues in seedling roots.

In principle, the incorporation of 3-*O*-propargylcaffeyl alcohol could also be detected by confocal Raman imaging at 2100 cm^{-1}, at which wavelength the terminal alkyne in our probe shows a significant peak but where biological systems typically have no scattering signals.[24,39] We envision that the incorporation of the designer monolignol along with click chemistry will enable the use of other imaging approaches, such as super-resolution microscopy,[44] to study the patterns and dynamics of lignification in plant cell walls.

To further demonstrate the utility of the designer monolignol, we performed incorporation experiments in stem sections of *Arabidopsis* Col-0 plants to test whether the designer monolignol could be assimilated into lignified cell walls. Forty-micron-thick stem cryosections of eight-week-old plants were incubated with 20 μM 3-*O*-propargylcaffeyl alcohol with 0.1 mg/mL HRP and labeled with Alexa 594-azide by the copper-catalyzed click reaction before imaging using confocal microscopy. The autofluorescence of both preexisting and newly formed lignins was detected using a 405 nm excitation laser, whereas incorporation of 3-*O*-propargylcaffeyl alcohol was detected by imaging Alexa 594-azide using 561 nm excitation. All stem sections showed 405-nm-excited autofluorescence specifically in lignifying tissues (Figure 5A–C), with higher autofluorescence intensities in vascular bundles compared to interfascicular fibers. Only stem sections treated with 3-*O*-propargylcaffeyl alcohol showed significant fluorescence in the 561 nm channel, with higher fluorescence appearing in interfascicular fibers than in vascular bundles. No visible fluorescence was observed in control stem sections that were treated with only coniferyl alcohol. These data are consistent with the result observed in the feeding experiment with live *Arabidopsis* seedlings, suggesting that lignin autofluorescence does not contribute to fluorescence imaging at 561 nm (also see Figure S2 in the Supporting Information). As seen in Figure 5D and E, fluorescence imaging at 405 and 561 nm allows for the differentiation of total (previously existing and newly formed) and newly formed lignins. Autofluorescence intensity increased insignificantly upon the addition of monolignols to the tissue (see Figure S3 in the Supporting Information), suggesting that it was mainly contributed by preexisting lignins in the xylem cells of vascular bundles (Figure 5D) and at the cell corners and middle lamellae in interfascicular fibers (Figure 5E). Regions of high fluorescence intensity at 561 nm, which correspond to the locations of newly formed lignin, were localized in inner wall layers and displayed barely detectable autofluorescence (Figure 5D,E). Together, these results indicate that the designer monolignol was successfully incorporated into lignified cell walls and is a substantially more sensitive method than autofluorescence for detecting new lignins. We envision that it will be very useful in revealing temporal and spatial details of lignification, which is crucial in understanding the molecular details of this intriguing process.

■ CONCLUSION

We have designed, synthesized, and tested 3-*O*-propargylcaffeyl alcohol as a designer monolignol and a coniferyl alcohol surrogate. Our data suggest that this compound is compatible with lignification and does not alter the fidelity of lignification. The incorporation of 3-*O*-propargylcaffeyl alcohol into lignins gives a unique Raman scattering signal in a cellularly silent

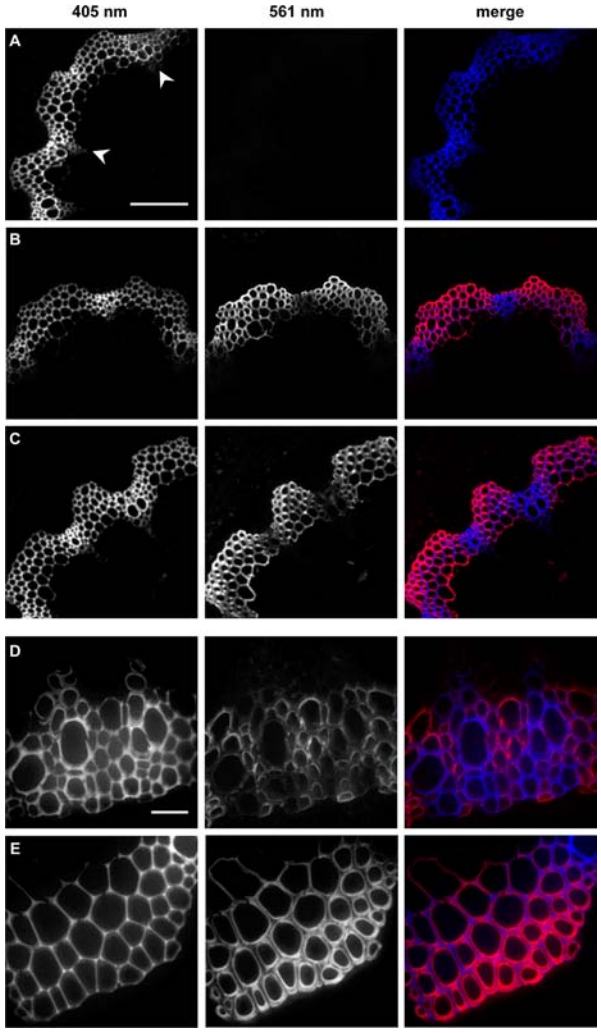

Figure 5. Autofluorescence (405 nm excitation) and click labeling (561 nm excitation) in 40-μm-thick sections of lignifying 8-week-old *Arabidopsis* stems. (A) Control section treated with 20 μM CA. (B) Section treated with 20 μM 3-*O*-propargylcaffeyl alcohol, **6**. (C) Section treated with 20 μM **6** and 20 μM CA. (D) Xylem and (E) interfascicular fibers (IFFs) of section treated with 20 μM **6** and 20 μM CA. Arrowheads in (A) indicate vascular bundles, with interfascicular fibers lying between bundles. Images are contrast-enhanced maximum intensity projections of *z* series recorded with a spinning disk fluorescence confocal microscope. (A–C) were recorded using a 20× objective with a 561 nm laser at 5% power, 150 gain, and 400 ms exposure time and a 405 nm laser at 100% power, 150 gain, and 400 ms exposure time (scale bar, 100 μm). (D,E) were recorded using a 63× objective with a 561 nm laser at 5% power, 10 gain, and 400 ms exposure time and a 405 nm laser at 100% power, 10 gain, and 400 ms exposure time (scale bar, 20 μm).

region. We further demonstrated that, when coupled with Alexa 594-azide using click chemistry, it generates strong fluorescence at 561 nm that is distinct from lignin autofluorescence and can be easily imaged. Our design sets up a general platform for using different spectroscopic and imaging approaches to interrogate plant cell wall lignification. We anticipate that a lignin spectroscopic toolbox on one "negligible" auxiliary for both in vitro and in vivo studies of lignification will shed new light on this complex and enigmatic polymer.

EXPERIMENTAL SECTION

General. Coniferyl alcohol was synthesized following published methods.[45] Horseradish peroxidase (type II, 150–250 units/mg), Alexa 594-azide, Murashige and Skoog salts, and Shandon Cryomatrix resin were purchased from Sigma-Aldrich, Life Technologies, Caisson Laboratories, and Thermo Scientific, respectively. Other commercial chemicals, including solvents, were of reagent grade or better, purchased from Sigma-Aldrich or Alfa Aesar, and used without further purification. Flash chromatography was performed using silica gel (230–450 mesh).

Nuclear Magnetic Resonance Spectroscopy. NMR spectra of small molecules (in acetone-d_6) and lignin DHPs [in dimethyl sulfoxide-d_6 (d_6-DMSO)] were obtained using standard Bruker pulse programs on a Bruker DPX-300 (300 MHz) spectrometer and a Bruker AV-III 500 (500 MHz) spectrometer with a cryogenically cooled gradient probe and inverse probe geometry (i.e., proton coils closest to sample), respectively. Spectral processing was performed using Bruker Topspin 3.1 software. Chemical shifts are reported in parts per million (ppm) using the central residual solvent peaks as internal references (δ_H/δ_C: acetone-d_6, 2.04/29.8 ppm; d_6-DMSO, 2.49/39.5 ppm). Fully authenticated assignments were made by the usual complement of 1D and 2D methods.[46,47]

Methyl 3-*O*-Propargylcaffeate. Methyl caffeate was prepared by adding caffeic acid (5.01 g, 27.8 mmol) and acetyl chloride (5.0 mL, 70 mmol) to 100 mL of methanol and stirring at room temperature overnight. The crude product (5.38 g) was obtained by removing the solvent under vacuum and was used in the following reaction without further purification. To a solution of methyl caffeate (1.91 g, 9.84 mmol) in anhydrous DMSO (300 mL) was added sodium hydride (60% in mineral oil, 0.806 g, 20.2 mmol) at 0 °C. The mixture was stirred at ambient temperature until no hydrogen gas was evolved. The mixture was then cooled to 0 °C before propargyl bromide (0.87 mL, 9.8 mmol) was added. The mixture was slowly warmed to room temperature overnight. The reaction was quenched by adding methanol (10 mL) at 0 °C. The mixture was extracted with ethyl acetate (200 mL × 4). The combined organic phase was washed consecutively with 1 M hydrochloric acid (200 mL), water (200 mL), and brine (200 mL); dried over magnesium sulfate; and concentrated under vacuum. The crude product was then carefully purified by column chromatography (25% to 40% ethyl acetate in hexanes), followed by recrystallization from ethyl acetate to give the desired methyl 3-*O*-propargylcaffeate (1.28 g, 56% yield) as a light yellow powder. ^{1}H NMR (acetone-d_6, 300 MHz) δ: 8.43 (1H, b, OH), 7.60 (1H, d, J = 15.9 Hz, H7), 7.44 (1H, d, J = 1.9 Hz, H2), 7.22 (1H, dd, J = 1.9 and 13.7 Hz, H6), 6.91 (1H, d, J = 13.7 Hz, H5), 6.41 (1H, d, J = 15.9 Hz, H8), 4.91 (2H, d, J = 2.4 Hz, propargyl CH_2), 3.72 (3H, s, CH_3), 3.12 (1H, t, J = 2.4 Hz, propargyl CH); ^{13}C NMR (acetone-d_6, 75 MHz) δ: 167.7 (C9), 150.4 (C4), 146.5 (C3) 145.4 (C7), 127.1 (C1), 124.7 (C6), 116.7 (C5), 115.7 (C8), 113.6 (C2), 79.4 (propargyl C), 77.3 (propargyl CH), 57.2 (propargyl CH_2), 52.0 (CH_3).

3-*O*-Propargylcaffeyl Alcohol. To a solution of methyl 3-*O*-propargylcaffeate (1.00 g, 4.56 mmol) in anhydrous tetrahydrofuran (30 mL) at 0 °C was added diisobutylaluminum hydride (DIBAL-H, 1.5 M in toluene, 12.2 mL, 18.2 mmol) over 1 h. The solution was stirred at 0 °C for an additional 30 min before quenching with ethyl acetate (30 mL).

dx.doi.org/10.1021/bc500411u | *Bioconjugate Chem.* 2014, 25, 2189–2196

To the mixture at 0 °C, half-saturated aqueous citric acid solution (60 mL) was added over a period of 30 min. The mixture was then stirred at ambient temperature for 3 h. The aqueous layer was extracted with ethyl acetate (100 mL × 3). The combined organic phase was washed with brine (100 mL), dried over magnesium sulfate, and concentrated under vacuum. The crude product was purified by column chromatography (50% ethyl acetate in hexanes) to give the desired product (0.85 g, 92% yield) as a pale-yellow solid. ^{1}H NMR (acetone-d_6, 300 MHz) δ 7.99 (1H, b, OH), 7.17 (1H, d, J = 1.8 Hz, H2), 6.93 (1H, dd, J = 1.8 and 8.0 Hz, H6), 6.83 (1H, d, J = 8.0 Hz, H5), 6.52 (1H, d, J = 15.9 Hz, Hα), 6.24 (1H, dt, J = 5.5 and 15.9 Hz, Hβ), 4.83 (2H, d, J = 2.4 Hz, propargyl CH_2), 4.24 (2H, d, J = 5.5 Hz, Hγ), 4.07 (1H, b, OH), 3.08 (1H, t, J = 2.4 Hz, propargyl CH); ^{13}C NMR (acetone-d_6, 75 MHz) δ 147.4 (C3), 146.2 (C4), 130.2 (Cα), 130.0 (C1), 128.0 (Cβ), 121.5 (C6), 116.4 (C5), 112.4 (C2), 79.7 (propargyl C), 77.0 (propargyl CH), 63.3 (Cγ), 57.2 (propargyl CH_2). HRMS (ESI) m/z calcd for $C_{12}H_{12}O_3$ $[M\text{-}H]^-$ 203.0708, found 203.0700.

Procedure for Producing Dehydrogenative Polymers (DHPs). A solution of 3-*O*-propargylcaffeyl alcohol (74 mg, 0.36 mmol), coniferyl alcohol (199 mg, 1.10 mmol), and methyl *p*-coumarate (5.2 mg, 0.029 mmol) in 5 mL of acetone was added dropwise to a solution of 10.8 M hydrogen peroxide (0.134 mL, 1.45 mmol) in 200 mL of sodium phosphate buffer (0.1 M, pH 6.5). Using a peristaltic pump, the resulting solution was added over 20 h to 20 mL of sodium phosphate buffer (0.1 M, pH 6.0) containing 3 mg of HRP. The reaction mixture was stirred for an additional 4 h. The precipitate was collected by centrifugation (12 000 *g*, 30 min), washed with ultrapure water (40 mL × 2), and dried under vacuum to give DHPs (0.162 g, 68%) as a yellow powder.

Raman Spectroscopy of DHPs. DHP polymers or copolymers were freeze-dried before spectrum acquisition. Raman spectra were collected using a Nicolet 8700 FT-Raman spectrometer. The dried DHP powder was excited using a diode-pumped 1064 nm Nd:YAG laser at 100 mW power and the signal was collected with a liquid nitrogen-cooled germanium detector. Fourier transform spectra were collected in the range 250−3500 cm^{-1} with data spacing of 1.928 cm^{-1} and were averaged from 500 scans. Raman spectra were baseline corrected and smoothed using the OMINIC spectra software (Thermo Scientific).

Incorporation, Labeling, and Imaging of *Arabidopsis* Seedlings. *Arabidopsis thaliana* seedlings of the Col-0 ecotype grown at 22 °C under 24 h light for 4 days were transferred from plates containing solid MS medium [2.2 g/L Murashige and Skoog salts, 0.6 g/L 2-(*N*-morpholino)ethanesulfonic acid, 8 g/L agar−agar, and 10 g/L sucrose, pH 5.6] to 1 mL liquid MS medium (MS medium lacking agar−agar) containing either 20 μM 3-*O*-propargylcaffeyl alcohol or 20 μM 3:1 coniferyl alcohol:3-*O*-propargylcaffeyl alcohol. Control seedlings were added to 1 mL liquid MS containing 20 μM coniferyl alcohol. Seedlings were incubated in constant light at 22 °C for 4 h. After incorporation, the seedlings were washed with liquid MS medium (1 mL × 4) and transferred to 1 mL of click-labeling solution containing 1 mM ascorbic acid, 1 mM $CuSO_4$, and 0.1 μM Alexa 594-azide in liquid MS. Labeling was performed at 25 °C in the dark with rocking for 1 h. Seedlings were washed with liquid MS (1 mL × 4) before imaging on a Zeiss Cell Observer SD spinning disk fluorescence confocal microscope using a 561 nm excitation laser and a 617/73 emission filter with a 20× 0.5 NA air immersion objective or a 100× 1.4 NA oil immersion objective. Maximum projections of collected z series were generated using ImageJ, adjusting image brightness equally for all images to maintain constant relative fluorescence intensities. Images were collected from a total of three replicate experiments with five seedlings imaged for each treatment.

Incorporation, Labeling, and Imaging of *Arabidopsis* Stem Sections. Middle portions of eight-week-old *Arabidopsis* Col-0 ecotype stems with secondary growth were cut into 8 mm pieces, embedded and frozen in Shandon Cryomatrix resin, cryosectioned into 40-μm-thick sections using a Leica CM1950 cryostat, and placed in water. Sections were then transferred to 1 mL aqueous solutions of 0.1 mg/mL HRP containing either 20 μM 3-*O*-propargylcaffeyl alcohol or 20 μM 3-*O*-propargylcaffeyl alcohol and 20 μM coniferyl alcohol. Control sections were added to 1 mL of aqueous solutions of 0.1 mg/mL HRP containing 20 μM coniferyl alcohol. These sections were incubated at 25 °C for 3 h. After incorporation, the sections were washed with water (1 mL × 4), transferred to 1 mL of click-labeling solution containing 1 mM ascorbic acid, 1 mM $CuSO_4$, and 1 μM Alexa 594-azide in liquid MS medium and rocked at 25 °C in the dark for 2 h. Sections were then washed with water (1 mL × 2), transferred to 1 mL of 96% ethanol, and rocked for 1 h to remove any unbound monomers or dyes before washing with water (1 mL × 4). Images were collected as above, with the addition of a 405 nm excitation laser and a 450/50 emission filter to image autofluorescence associated with lignin and a 63× 1.4 NA oil immersion objective. Maximum projections of z series were generated using ImageJ, adjusting image brightness equally for all images to maintain constant relative fluorescence intensities. Fluorescence intensities were quantified as raw integrated intensities per unit area using ImageJ after using a common threshold for the images to be compared to select lignified regions. Separate threshold regions were set for images acquired under the 405 and 561 nm channels. Images were collected from a total of three replicate experiments with three sections imaged for each treatment.

■ ASSOCIATED CONTENT

Ⓢ Supporting Information

NMR spectra of all compounds, autofluorescence and click labeling of untreated *Arabidopsis* stem sections, quantification of fluorescence intensities of *Arabidopsis* stem sections. This material is available free of charge via the Internet at http://pubs.acs.org.

■ AUTHOR INFORMATION

Corresponding Author

*E-mail: yuz30@psu.edu.

Author Contributions

Natalie Bukowski and Jyotsna L. Pandey contributed equally to this work.

Notes

The authors declare no competing financial interest.

■ ACKNOWLEDGMENTS

We thank Sarah Kiemle for advice on cryosectioning, which was performed at the Penn State Microscopy and Cytometry Facility - University Park, PA. This work is financially supported by Penn State Altoona Research Development Grant (to Y.Z.) and the Center for Lignocellulose Structure and Formation, an

Energy Frontier Research Center funded by the U.S. Department of Energy, Office of Science, Basic Energy Sciences under Award # DE-SC0001090 (to T.R. and C.T.A.).

REFERENCES

(1) Boerjan, W., Ralph, J., and Baucher, M. (2003) Lignin biosynthesis. *Annu. Rev. Plant Biol. 54*, 519−546.
(2) Bonawitz, N. D., and Chapple, C. (2010) The genetics of lignin biosynthesis: Connecting genotype to phenotype. *Annu. Rev. Genet. 44*, 337−363.
(3) Vanholme, R., Demedts, B., Morreel, K., Ralph, J., and Boerjan, W. (2010) Lignin biosynthesis and structure. *Plant Physiol. 153*, 895−905.
(4) Bonawitz, N. D., and Chapple, C. (2013) Can genetic engineering of lignin deposition be accomplished without an unacceptable yield penalty? *Curr. Opin. Biotechnol. 24*, 336−343.
(5) Ragauskas, A. J., Beckham, G. T., Biddy, M. J., Chandra, R., Chen, F., Davis, M. F., Davison, B. H., Dixon, R. A., Gilna, P., Keller, M., Langan, P., Naskar, A. K., Saddler, J. N., Tschaplinski, T. J., Tuskan, G. A., and Wyman, C. E. (2014) Lignin valorization: improving lignin processing in the biorefinery, *Science 344*, DOI: 10.1126/science.1246843.
(6) Vanholme, R., Morreel, K., Ralph, J., and Boerjan, W. (2008) Lignin engineering. *Curr. Opin. Plant Biol. 11*, 278−285.
(7) Bonawitz, N. D., Kim, J. I., Tobimatsu, Y., Ciesielski, P. N., Anderson, N. A., Ximenes, E., Maeda, J., Ralph, J., Donohoe, B. S., Ladisch, M., and Chapple, C. (2014) Disruption of mediator rescues the stunted growth of a lignin-deficient *Arabidopsis* mutant. *Nature 509*, 376−380.
(8) Mansfield, S. D., Kang, K.-Y., and Chapple, C. (2012) Designed for deconstruction - Poplar trees altered in cell wall lignification improve the efficacy of bioethanol production. *New Phytol. 194*, 91−101.
(9) Vanholme, R., Morreel, K., Darrah, C., Oyarce, P., Grabber, J. H., Ralph, J., and Boerjan, W. (2012) Metabolic engineering of novel lignin in biomass crops. *New Phytol. 196*, 978−1000.
(10) Simmons, B. A., Loque, D., and Ralph, J. (2010) Advances in modifying lignin for enhanced biofuel production. *Curr. Opin. Plant Biol. 13*, 313−320.
(11) Wilkerson, C. G., Mansfield, S. D., Lu, F., Withers, S., Park, J. Y., Karlen, S. D., Gonzales-Vigil, E., Padmakshan, D., Unda, F., Rencoret, J. R., and Ralph, J. (2014) Monolignol ferulate transferase introduces chemically labile linkages into the lignin backbone. *Science 344*, 90−93.
(12) Wang, J. P., Naik, P. P., Chen, H. C., Shi, R., Lin, C. Y., Liu, J., Shuford, C. M., Li, Q., Sun, Y. H., Tunlaya-Anukit, S., Williams, C. M., Muddiman, D. C., Ducoste, J. J., Sederoff, R. R., and Chiang, V. L. (2014) Complete proteomic-based enzyme reaction and inhibition kinetics reveal how monolignol biosynthetic enzyme families affect metabolic flux and lignin in Populus trichocarpa. *Plant Cell 26*, 894−914.
(13) Vanholme, R., Cesarino, I., Rataj, K., Xiao, Y., Sundin, L., Goeminne, G., Kim, H., Cross, J., Morreel, K., Araujo, P., Welsh, L., Haustraete, J., McClellan, C., Vanholme, B., Ralph, J., Simpson, G. G., Halpin, C., and Boerjan, W. (2013) Caffeoyl shikimate esterase (CSE) is an enzyme in the lignin biosynthetic pathway in *Arabidopsis*. *Science 341*, 1103−1106.
(14) Liu, C.-J. (2012) Deciphering the enigma of lignification: Precursor transport, oxidation, and the topochemistry of lignin assembly. *Mol. Plant 5*, 304−317.
(15) Wang, Y., Chantreau, M., Sibout, R., and Hawkins, S. (2013) Plant cell wall lignification and monolignol metabolism. *Front. Plant Sci. 4*, 220.
(16) Achyuthan, K. E., Achyuthan, A. M., Adams, P. D., Dirk, S. M., Harper, J. C., Simmons, B. A., and Singh, A. K. (2010) Supramolecular self-assembled chaos: Polyphenolic lignin's barrier to cost-effective lignocellulosic biofuels. *Molecules 15*, 8641−8688.
(17) Miao, Y.-C., and Liu, C.-J. (2010) ATP-binding cassette-like transporters are involved in the transport of lignin precursors across plasma and vacuolar membranes. *Proc. Natl. Acad. Sci. U. S. A. 107*, 22728−22733.
(18) Alejandro, S., Lee, Y., Tohge, T., Sudre, D., Osorio, S., Park, J., Bovet, L., Lee, Y., Geldner, N., Fernie, A. R., and Martinoia, E. (2012) AtABCG29 is a monolignol transporter involved in lignin biosynthesis. *Curr. Biol. 22*, 1207−1212.
(19) Sibout, R., and Hofte, H. (2012) Plant cell biology: The ABC of monolignol transport. *Curr. Biol. 22*, R533−R535.
(20) Lee, Y., Rubio, M. C., Alassimone, J., and Geldner, N. (2013) A mechanism for localized lignin deposition in the endodermis. *Cell 153*, 402−412.
(21) Zhao, Q., Nakashima, J., Chen, F., Yin, Y., Fu, C., Yun, J., Shao, H., Wang, X., Wang, Z. Y., and Dixon, R. A. (2013) Laccase is necessary and nonredundant with peroxidase for lignin polymerization during vascular development in *Arabidopsis*. *Plant Cell 25*, 3976−3987.
(22) Gierlinger, N., and Schwanninger, M. (2006) Chemical imaging of poplar wood cell walls by confocal Raman microscopy. *Plant Physiol. 140*, 1246−1254.
(23) Tsien, R. Y. (2009) Constructing and exploiting the fluorescent protein paintbox. *Angew. Chem., Int. Ed. 48*, 5612−5626.
(24) Schmidt, M., Schwartzberg, A. M., Carroll, A., Chaibang, A., Adams, P. D., and Schuck, P. J. (2010) Raman imaging of cell wall polymers in *Arabidopsis thaliana*. *Biochem. Biophys. Res. Commun. 395*, 521−523.
(25) Chudakov, D. M., Matz, M. V., Lukyanov, S., and Lukyanov, K. A. (2010) Fluorescent proteins and their applications in imaging living cells and tissues. *Physiol. Rev. 90*, 1103−1163.
(26) Lee, K. J., Marcus, S. E., and Knox, J. P. (2011) Cell wall biology: Perspectives from cell wall imaging. *Mol. Plant 4*, 212−219.
(27) Flors, C. (2013) Super-resolution fluorescence imaging of directly labelled DNA: From microscopy standards to living cells. *J. Microsc. 251*, 1−4.
(28) Shieh, P., Siegrist, M. S., Cullen, A. J., and Bertozzi, C. R. (2014) Imaging bacterial peptidoglycan with near-infrared fluorogenic azide probes. *Proc. Natl. Acad. Sci. U. S. A. 111*, 5456−5461.
(29) Laughlin, S. T., and Bertozzi, C. R. (2009) Imaging the glycome. *Proc. Natl. Acad. Sci. U. S. A. 106*, 12−17.
(30) Rouhanifard, S. H., Nordstrom, L. U., Zheng, T., and Wu, P. (2013) Chemical probing of glycans in cells and organisms. *Chem. Soc. Rev. 42*, 4284−4296.
(31) Tobimatsu, Y., Davidson, C. L., Grabber, J. H., and Ralph, J. (2011) Fluorescence-tagged monolignols: Synthesis, and application to studying in vitro lignification. *Biomacromolecules 12*, 1752−1761.
(32) Tobimatsu, Y., Wagner, A., Donaldson, L., Mitra, P., Niculaes, C., Dima, O., Kim, J. I., Anderson, N., Loque, D., Boerjan, W., Chapple, C., and Ralph, J. (2013) Visualization of plant cell wall lignification using fluorescence-tagged monolignols. *Plant J. 76*, 357−366.
(33) Tobimatsu, Y., Wagner, A., Donaldson, L., Mitra, P., Loque, D., Dima, O., Niculaes, C., Boerjan, W., Kim, J. I., Anderson, N., Chapple, C., Schuetz, M., Takano, T., Nakatsubo, F., and Ralph, J. (2014) Synthetic monolignol mimics for understanding lignin biosynthesis, *Abstracts of Papers*, 247th ACS National Meeting & Exposition, Dallas, TX, United States, March 16−20, 2014, CELL-185.
(34) Sletten, E. M., and Bertozzi, C. R. (2009) Bioorthogonal Chemistry: Fishing for selectivity in a sea of functionality. *Angew. Chem., Int. Ed. 48*, 6974−6998.
(35) Anderson, C. T., and Wallace, I. S. (2012) Illuminating the wall: using click chemistry to image pectins in Arabidopsis cell walls. *Plant Signaling Behav. 7*, 661−663.
(36) Rostovtsev, V. V., Green, L. G., Fokin, V. V., and Sharpless, K. B. (2002) A stepwise Huisgen cycloaddition process: Copper(I)-catalyzed regioselective "ligation" of azides and terminal alkynes. *Angew. Chem., Int. Ed. 41*, 2596−2599.
(37) Tornoe, C. W., Christensen, C., and Meldal, M. (2002) Peptidotriazoles on solid phase: [1,2,3]-Triazoles by regiospecific copper(I)-catalyzed 1,3-dipolar cycloadditions of terminal alkynes to azides. *J. Org. Chem. 67*, 3057−3064.

(38) Yamakoshi, H., Dodo, K., Palonpon, A., Ando, J., Fujita, K., Kawata, S., and Sodeoka, M. (2012) Alkyne-tag Raman imaging for visualization of mobile small molecules in live cells. *J. Am. Chem. Soc. 134*, 20681−20689.
(39) Palonpon, A. F., Ando, J., Yamakoshi, H., Dodo, K., Sodeoka, M., Kawata, S., and Fujita, K. (2013) Raman and SERS microscopy for molecular imaging of live cells. *Nat. Protoc. 8*, 677−692.
(40) Syrjanen, K., and Brunow, G. (1998) Oxidative cross coupling of *p*-hydroxycinnamic alcohols with dimeric arylglycerol *β*-aryl ether lignin model compounds. The effect of oxidation potentials. *J. Chem. Soc., Perkin Trans. 1*, 3425−3430.
(41) Grabber, J. H., Hatfield, R. D., Lu, F., and Ralph, J. (2008) Coniferyl ferulate incorporation into lignin enhances the alkaline delignification and enzymatic degradation of cell walls. *Biomacromolecules 9*, 2510−2516.
(42) Grabber, J. H., Schatz, P. F., Kim, H., Lu, F., and Ralph, J. (2010) Identifying new lignin bioengineering targets: 1. Monolignol-substitute impacts on lignin formation and cell wall fermentability. *BMC Plant Biol. 10*, 1−13.
(43) Lu, F., and Ralph, J. (2008) Novel tetrahydrofuran structures derived from *β*-*β*-coupling reactions involving sinapyl acetate in Kenaf lignins. *Org. Biomol. Chem. 6*, 3681−3694.
(44) Zessin, P. J., Finan, K., and Heilemann, M. (2012) Super-resolution fluorescence imaging of chromosomal DNA. *J. Struct. Biol. 177*, 344−348.
(45) Kim, H., and Ralph, J. (2005) Simplified preparation of coniferyl and sinapyl alcohols. *J. Agric. Food Chem. 53*, 3693−3695.
(46) Lu, F., and Ralph, J. (2011) Solution-state NMR of lignocellulosic biomass. *J. Biobased Mater. Bioenergy 5*, 169−180.
(47) Mansfield, S. D., Kim, H., Lu, F., and Ralph, J. (2012) Whole plant cell wall characterization using solution-state 2D NMR. *Nat. Protoc. 7*, 1579−1589.

■ NOTE ADDED IN PROOF

After we submitted this manuscript, Ralph and co-workers published a similar click chemistry strategy for interrogation of plant cell wall lignification, in which the designed monolignols were modified at the *γ*-*O*-site instead of the 3-*O*-position reported in this work. See: Tobimatsu, Y., Van de Wouwer, D.; Allen, E.; Kumpf, R., Vanholme, B., Boerjan, W., and Ralph, J. (2014) A click chemistry strategy for visualization of plant cell wall lignification, *Chem. Commun.* doi: 10.1039/C4CC04692G.